Ecotoxicology and Environmental Safety 291 (2025) 117821

Contents lists available at ScienceDirect

Ecotoxicology and Environmental Safety

journal homepage: www.elsevier.com/locate/ecoenv

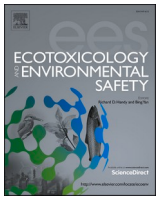

Sodium butyrate attenuates oxidative stress, apoptosis, and excessive mitophagy in sodium fluoride-induced hepatotoxicity in rats

Jing Xia [a,1], Xiaolin Zhang [b,1], Leiyu Xu [a], Nan Yan [c], Zhenxiang Sun [a], Xiaoxu Duan [d], Lu Meng [a], Rong Qi [e], Fu Ren [a,*], Zhengdong Wang [a,*]

[a] Liaoning Province Key Laboratory for phenomics of Human Ethnic Specificity and Critical Illness, Shenyang Medical College, Shengyang, PR China
[b] Department of General Surgery, Central Hospital Affiliated to Shenyang Medical College, Shengyang, PR China
[c] Rehabilitation Medical Scool, Shenyang Medical College, Shengyang, PR China
[d] School of Public Health College, Shenyang Medical College, Shenyang, PR China
[e] Laboratory of Molecular Morphology, Basic Medical College, Shenyang Medical College, Shengyang, PR China

ARTICLE INFO

Edited by Dr. Caterina Faggio

Keywords:
Fluorosis
Liver
Mitophagy
Sodium butyrate
Sodium fluoride

ABSTRACT

Aim: Long-term exposure to excess sodium fluoride (NaF) can cause chronic fluorosis. Liver, the most important detoxification organ, is the most vulnerable to the effects of fluoride. Sodium butyrate (NaB), a short-chain fatty acid produced in the intestinal tract, maintains normal mitochondrial function in vivo and reduces liver inflammation and oxidative stress. This study aims to investigate the protective effect and potential mechanism of NaB on liver injury in fluoride poisoned rats, particularly through the mitophagy pathway.

Methods: Rats were randomly divided into four groups of 12 male rats each: control, NaF (100 mg/mL), NaB (1000 mg/kg), and NaF (100 mg/mL)+NaB (1000 mg/kg) group.

Key findings: Changes in the levels of liver enzymes (alanine aminotransferase [ALT] and aspartate aminotransferase [AST]) and antioxidant enzymes (superoxide dismutase [SOD], catalase [CAT], and malondialdehyde [MDA]) confirmed NaF-induced liver injury. NaF also changed the levels of autophagy markers (Beclin-1, LC3α/β, P62), and increased the level of apoptosis. The combined use of NaB and NaF significantly ameliorated these indices.

Significance: These findings indicate that NaB may provide effective protection against NaF-induced liver injury through its attenuates oxidative stress, apoptosis, and excessive mitophagy mechanisms.

1. Introduction

Fluorine, which is abundantly found in nature and widely utilized in industry and agriculture, serves as an essential trace element for human growth and development. Furthermore, moderate exposure to fluoride has been shown to aid in the prevention of dental caries (O'mullane et al., 2016). The World Health Organization recommends a maximum fluoride concentration of 1.5 mg/L in drinking water. However, fluoride concentrations in drinking water in many regions of the world have exceeded this standard, with some areas even reaching as high as 40 mg/L (Hung et al., 2023; Aguilar-Díaz et al., 2017; Feng et al., 2020). Consequently, symptoms of chronic fluorosis have been observed within the local population. It is estimated that more than 200 million individuals worldwide are at risk of fluorosis (Liu et al., 2024).

Studies have shown that excessive fluoride intake results in its accumulation in the body, adversely affecting both the skeletal and non-skeletal systems. The accumulation of NaF alters bone density, resulting in dental fluorosis and skeletal fluorosis (Smith, 1988; Martignon et al., 2021). Overconsumption of fluoride also causes detrimental effects on the nervous and gastrointestinal systems, leading to inflammation and oxidative stress (Waugh, 2019; Wang et al., 2020; Li et al., 2023). Recent studies have further demonstrated that intake of excessive amounts of fluoride impairs cognitive function by affecting brain health (Duan et al., 2018), and it can also lead to degenerative eye diseases such as

* Corresponding authors.
E-mail addresses: 15138246090@163.com (J. Xia), zzyzxm20142019@163.com (X. Zhang), xly13359823027@163.com (L. Xu), yannan@symc.edu.cn (N. Yan), sunqi1226@symc.edu.cn (Z. Sun), duanxiaoxu@symc.edu.cn (X. Duan), ml19176969779@163.com (L. Meng), qlrr@symc.edu.cn (R. Qi), rf@symc.edu.cn (F. Ren), wangzhengdong@symc.edu.cn (Z. Wang).
[1] Jing Xia and Xiaolin Zhang contributed equally to the study and should be considered co-first authors.

https://doi.org/10.1016/j.ecoenv.2025.117821
Received 24 November 2024; Received in revised form 20 January 2025; Accepted 27 January 2025
Available online 30 January 2025
0147-6513/© 2025 The Author(s). Published by Elsevier Inc. This is an open access article under the CC BY-NC-ND license (http://creativecommons.org/licenses/by-nc-nd/4.0/).

cataracts and macular degeneration through the disruption of eye-related molecular mechanisms (Waugh, 2019). Most importantly, because toxic substances must be metabolized by the liver and excreted through the kidneys, the liver and kidneys are particularly susceptible to fluoride damage.

Liver is the body's largest detoxification organ, and overexposure to fluoride can induce oxidative stress and mitochondrial damage (Zong et al., 2023; Song et al., 2023). Excessive NaF is absorbed by the liver, it triggers the overproduction of reactive oxygen species (ROS), which attack the mitochondria, leading to mitochondrial dysfunction. Subsequently, the mitochondria lose their membrane potential, and cytochrome C is released from the inner membrane into the cytoplasm, triggering apoptosis. Fortunately, when dysfunctional mitochondria are detected within the cell, mitophagy is spontaneously activated to remove the abnormal mitochondria and restore mitochondrial homeostasis, thereby regulating intracellular redox balance and preventing cellular damage induced by oxidative stress (Tian et al., 2025).

In recent years, an increasing number of researchers have recognized mitophagy as a potential therapeutic target for fluorosis. Mitochondria are the primary energy-producing organelles and serve as the principal source of ROS production. Mitochondrial dysfunction results in the overproduction of ROS, thereby disrupting the redox balance in the body and triggering systemic oxidative stress. It has been shown that oxidative stress activates the mitophagy mechanism, selectively packaging dysfunctional or excess mitochondria into autophagosomes, which are then transported to the lysosome for degradation, thereby regulating mitochondrial number and maintaining cellular energy metabolism stability (Gu et al., 2024; Garza-Lombó et al., 2020). Several studies have illustrated that excessive fluoride intake results in mitochondrial dysfunction and disrupts the balance of mitophagy (Wang et al., 2024). Fluoride has been demonstrated to cause neurotoxicity by inducing abnormal mitophagy (Dong et al., 2024). Excessive mitophagy induced by NaF can also be inhibited through calcium ion supplementation, thereby alleviating bone tissue damage (Hu et al., 2024). It has also been shown that alpha-lipoic acid can mitigate NaF -induced liver injury by enhancing antioxidant capacity while improving mitochondrial function (Yu et al., 2023).

Theoretically, fluorosis can be effectively treated by reducing mitochondrial dysfunction and enhancing cellular resistance to oxidative stress. NaB is a short-chain fatty acid synthesized in the intestine, produced by the fermentation of fibrous bacteria in the colon. It naturally exists in the body, characterized by low toxicity and high efficiency. Multiple studies have proved that NaB possesses a variety of physiological activities, including antioxidant effects, regulation of mitophagy (Xue et al., 2023; Li et al., 2022), maintenance of intestinal microbial homeostasis (Zhou et al., 2017), and exertion of anti-inflammatory effects (Chang et al., 2014; Park et al., n.d.). Studies have confirmed that NaB is effective in alleviating alcoholic liver disease by decreasing oxidative stress levels, through adjusting Nrf2 signaling (Watchon et al., 2024; Wen et al., 2024). It also significantly improves non-alcoholic fatty liver disease induced by a high-fat diet through antioxidant effects. Research has demonstrated that NaB has potential clinical application value in the treatment of liver diseases. Evidence suggests that NaB can improve neurological function by modulating mitophagy, highlighting its therapeutic potential, while its mitochondria-related molecular mechanisms in the treatment of liver diseases require further clarification.

2. Materials and methods

2.1. Chemicals

NaF and NaB were purchased from MACKLIN Biological Reagent (Shanghai, China). Reagents such as BCA, RIPA, and PMSF were procured from Beijing Dingguo Changsheng Biotechnology (Shenyang, China). Kits for assessing rat liver function and oxidative stress were obtained from Nanjing Jiancheng (Nanjing, China). The antibodies utilized for western blot analysis were acquired from Wanlei Biotechnology (Shenyang, China).

2.2. Animal

48 male SD rats (4 weeks old, weighing 250–280 g) were purchased from Beijing HFK Biotechnology (Beijing, China). These rats were maintained under standardized laboratory settings, which included a 12-hour light/dark cycle, a temperature of 24 ± 1°C, and a humidity level of 45 ± 5 %, animals were housed in plastic cages. Free access to food and water was provided. Animal experiments were approved by the Animal Experiment Ethics Committee of Shenyang Medical College (No. SYYXY2023051001).

2.3. Experimental design

The animals were randomly assigned to four groups, each consisting of 12 rats: Control, NaF, NaB, and NaF + NaB group. Rats in the NaF, NaF + NaB groups were given free access to 100 mg/L fluorine-containing distilled water daily, whereas rats in the Control and NaB groups were given only distilled water. Three months after fluoride exposure, the Rats in the NaB and NaF + NaB groups are intragastrically administered 1000 mg/kg NaB daily. Rats in the Control and NaF groups were intragastrically administered equal doses of physiological saline for 4 weeks, feeding fluorine concentration remaining unchanged in drinking water (Li et al., 2023). At the end of week 17, the rats were euthanized with an intraperitoneal injection of 200 mg/kg pentobarbital sodium. The blood was centrifuged at 3000 rpm for 10 min to separate the serum. Liver function and serum fluoride levels were then detected. The rats were placed in metabolic cages, and water was withheld for 24 h to collect urine. Urine fluoride levels were detected using the collected urine samples. Liver tissue was stored in a −80°C freezer. Three rats from each group were fixed via cardiac perfusion with 4 % paraformaldehyde after flushing out red blood cells.

2.4. Fluoride ion selective electrode

The fluoride content in the urine and serum was determined using a fluoride ion-selective electrode. Rat urine was collected by the metabolic cage, and following euthanasia, abdominal aortic blood was collected and centrifuged at 3000 rpm for 10 min to separate the serum. The ion meter was calibrated using standard fluoride ion solutions of varying concentrations (Thunder Magnetic Instruments, Shanghai, China). The samples were diluted in a 1:1 ratio with a total ion concentration buffer solution (Thunder Magnetic Instruments, Shanghai, China) and the average concentration was measured using the fluoride ion meter.

2.5. Serum biochemical analysis

AST、ALT were measured in serum samples prepared from blood collected after 4 weeks of treatment. Utilize commercially available reagent kits for testing (Nanjing Jiancheng Bioengineering Research Institute, Nanjing, China). Samples and standards were processed according to the manufacturer's instructions.

2.6. Measurement of antioxidant and oxidative damage parameters

The liver of the rat was homogenized at a ratio of 1:9 (weight [g]: deionized water volume [mL]). After centrifugation at the specified speed, the supernatant was transferred to a new centrifuge tube. The levels of oxidative stress markers, including malondialdehyde (MDA) and antioxidant enzymes (SOD, CAT), were measured according to the detailed procedures provided in the kit instructions (Nanjing Jiancheng Bioengineering Institute, China). Additionally, protein concentrations were determined using a BCA protein assay kit (Beijing Dingguo,

Shenyang, China).

2.7. Western blotting analysis

Rat liver tissue was homogenized in a RIPA buffer containing PMSF (DingGuo ChangSheng Biotechnology, Shenyang, China) at a ratio of 100:1 to extract total protein. Protein concentrations in the liver samples were determined using a BCA assay kit (DingGuo ChangSheng Biotechnology, Shenyang, China). Equal amounts of protein (45 μg) were separated by 8–12 % SDS-PAGE and transferred to a PVDF membrane (Merck Millipore, USA). The membrane was blocked with 5 % milk powder at room temperature for 2 h, then incubated overnight at 4°C with primary antibodies: LC3 (1:1500; Wanleibio, China), p62 (1:2000; Wanleibio, China), Beclin-1 (1:1500; Wanleibio, China), GAPDH (1:5000; ABclonal, USA), and β-actin (1:2000; ABclonal, USA). After washing with TBST, goat anti-rabbit IgG conjugated with horseradish peroxidase (1:7000; DingGuo ChangSheng Biotechnology, Shenyang, China) was added to the wash solution and incubated for 2 h at room temperature. The membrane was then treated with an ECL luminescent solution (Biyun Tian, Dalian, China) and imaged using a ChemiDoc multifunctional imaging system. Signal intensities were quantified using ImageJ 1.4 software (Bethesda, Maryland, USA).

2.8. Gene expression analysis

Liver samples were collected for RNA extraction. Total RNA was extracted using an RNA extraction kit (Magen, Guangzhou, China). cDNA was synthesized from the total RNA using a cDNA Reverse Transcription Kit (Takara Biomedical Technology, Dalian, China). Real-time PCR was performed using a Bio-Rad CFX96 Connect Real-time PCR System (Bio-Rad, USA). GAPDH, a housekeeping gene, was used for normalization and relative quantification. The corresponding primer sequences are listed in Table 1. The relative quantitative analysis of the target gene was performed using the $2^{-\Delta\Delta Ct}$ method.

2.9. Histopathological analysis

Liver samples from the four experimental groups were fixed in a 4 % paraformaldehyde solution and subsequently embedded in paraffin. Hematoxylin-eosin (H&E) staining was performed following standard protocols. Image analysis was conducted using an optical microscope (Motic, Xiamen, China).

2.10. Transmission electron microscopy

Liver tissue (about 1 mm^3) was fixed for 2 h at 4°C in 4 % paraformaldehyde and 0.1 mol/L phosphate buffer (pH 7.3), supplemented with 2.5 % glutaraldehyde. The tissue was thoroughly rinsed with the same phosphate buffer and subsequently fixed in a 1 % osmium tetroxide solution, with 0.1 mol/L phosphate buffer (pH 7.3). After fixation, the tissue was dehydrated in ethanol, embedded in, and cut using a microtome. The sections were stained with 1 % uranyl acetate to enhance contrast. Finally, the samples were observed using a transmission electron microscope (JEM-2000 EXII, 80 KV, Japan).

2.11. Apoptosis

Apoptosis in rat liver cells was assessed using TUNEL staining with the TUNEL Cell Apoptosis Detection Kit POD (Doctoral Bioengineering Co., Ltd., Wuhan, China). The process was conducted strictly according to the provided operational instructions. The samples were then observed under an optical microscope.

2.12. Statistical analysis

Data are expressed as mean ± standard deviation. Statistical analyses were performed using the GraphPad Prism 8 software (San Diego, CA, USA). Comparisons between multiple groups were conducted using one-way ANOVA variance with at least three replicates for each group. Differences were considered statistically significant at * $P < 0.05$, ** $P < 0.01$, and *** $P < 0.001$.

3. Results

3.1. Incidence of dental fluorosis in rats

To verify the successful establishment of the model, we calculated the incidence of dental fluorosis in each group of rats and monitored their growth status. The results are presented in Table 2. The lower incisors of rats in the control and NaB groups had normal morphology. Compared to the control group, the incidence of dental fluorosis significantly increased after NaF treatment. In the NaF group, the teeth became elongated and malformed, with the tips of the teeth growing laterally. In addition, the fur of the rats in the NaF group was rough and messy, with loss of appetite, depression, and reduced frequency of activity. Compared with the NaF treatment group, the incidence of dental fluorosis of the NaF +NaB group showed a 10 % decrease of dental fluorosis, the roughness of the fur and mental state improved, and the number of activities increased significantly.

3.2. Effects of NaF and NaB on liver weight and liver-brain coefficient

Quickly weigh the liver and whole brain weight after extracting tissues from rats, and calculate their ratio. The liver weight and liver-brain coefficient of each group of rats are shown in Table 3. Compared with the control group, the liver weight and liver-brain coefficient of rats in the NaF group were significantly lower ($p < 0.01$), indicating that the rat livers were atrophied and showed degenerative changes. The liver weight and liver-brain ratio of rats in the NaF + NaB group significantly improved ($p < 0.01$) compared with those in the NaF group.

3.3. Effects of NaF and NaB on fluoride ion concentration in serum and urine

Using the fluoride ion selective electrode method detected the fluoride ion concentration in serum and urine. The detection results are shown in Table 4. The fluoride ion concentration in the serum and urine of rats in the NaF group was significantly higher than that in the control group ($p < 0.001$), whereas the fluoride ion concentration in the blood and urine of rats in the NaF + NaB group were improved compared to the NaF group ($p < 0.05$).

Table 1
Primer base sequence of RT-qPCR detection.

Gene	Forward primer sequences (5′-3′)	Reverse primer sequences (5′-3′)
Beclin−1	AACTCTGGAGGTCTCGCTCT	CGCCTTAGACCCCTCCATTC
LC3B	CCAGTGATTATAGAGCGATACAAGG	AGGAGGAAGAAGGCTTGGTTAG
P62	GGAAGCTGAAACATGGGCAC	TGGGATCCTCTGATGGAGCA
GAPDH	ACAGCAACAGGGTGGTGGAC	TTTGAGGGTGCAGCGAACTT

Table 2
Effect of NaF and NaB administration on the incidence of dental fluorosis in rats.

Group	Quantity	Occurrence of dental fluorosis (pieces)				Total number of occurrences	detection rat%
		normal	1degree	2degree	3degree		
Control	10	10	0	0	0	0	0
NaB	10	10	0	0	0	0	0
NaF	10	0	1	7	2	10	100
NaF +NaB	10	1	4	4	1	9	90

Table 3
Effect of NaF and NaB administration on liver weight, liver coefficient, blood fluoride, and urine fluoride levels.

Group	Absolute liver weights (g)	Relative liver weights (mg/g)	Serum fluoride concentration (mg/L)	Urine fluoride concentration (mg/L)
Control	10.38 ± 0.300	5.00 ± 0.105	0.1110 ± 0.005	1.715 ± 0.090
NaB	9.11 ± 0.339	4.52 ± 0.126	0.1030 ± 0.010	1.519 ± 0.124
NaF	7.46 ± 0.402**	3.90 ± 0.095**	0.1565 ± 0.007***	8.139 ± 0.348****
NaF +NaB	9.58 ± 0.326$^{\#\#}$	4.70 ± 0.175$^{\#\#}$	0.1289 ± 0.004$^{\#}$	6.794 ± 0.549$^{\#}$

Note: Data are expressed as mean ± SEM (n = 6). ** $P < 0.01$, *** $P < 0.001$, **** $P < 0.0001$ compared with group C; $^{\#}$ $P < 0.05$, $^{\#\#}$ $P < 0.01$, compared with NaF group.

Table 4
Effects of NaB and NaF administrations on hepatic serum levels (ALT, AST) and oxidative stress biomarkers (MDA, CAT and SOD).

Group	AST(U/L)	ALT(U/L)	MDA (nmol/g tissue)	CAT (katal/g protein)	SOD (U/g protein)
Control	3.22 ± 0.80	14.63 ± 3.12	0.568 ± 0.078	26.67 ± 3.96	248.9 ± 16.94
NaB	4.53 ± 0.84	12.4 ± 1.09	0.383 ± 0.108	30.81 ± 2.84	229.4 ± 17.87
NaF	11.86 ± 0.67**	40.91 ± 4.18**	1.133 ± 0.123**	10.01 ± 0.90**	163.8 ± 10.56**
NaF +NaB	3.31 ± 0.57$^{\#\#}$	12.57 ± 1.63$^{\#\#}$	0.558 ± 0.066$^{\#}$	33.03 ± 2.45$^{\#\#}$	254.3 ± 27.98$^{\#\#}$

Note: Data are expressed as mean ± SEM (n = 6). ** $P < 0.01$, compared with group C; $^{\#\#}$ $P < 0.01$, compared with NaF group.

3.4. Effects of NaF and NaB on liver tissue pathological damage

To investigate the pathological damage induced by NaF in rat liver tissue and the effects of NaB on this damage, histopathological changes in rat liver tissue were further observed under a light microscope. As shown in Fig. 1, a normal histological structure was observed in the control and NaB-treated groups. The liver structure was clear, and the hepatocytes were neatly arranged and closely packed. The NaF group had a disorganized arrangement of hepatocytes and a large amount of vacuolar degeneration and inflammatory infiltration, which is a manifestation of severe liver tissue damage, whereas the NaF + NaB group showed a neatly arranged arrangement of hepatocytes, a reduction in inflammatory infiltration, and an improvement in vacuolar degeneration.

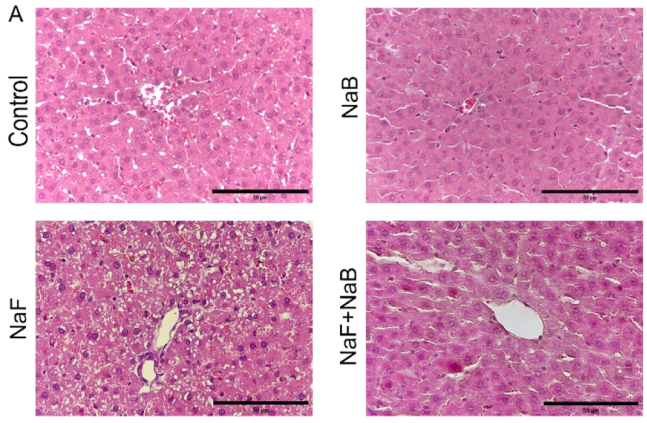

Fig. 1. Effects of NaF and NaB on histopathological changes. The liver tissue sections of four groups of rats are shown in the figure, and the Control and NaB groups of rats exhibit normal histological appearance; NaF group shows enlargement of central veins and hepatic sinusoids, irregular cell arrangement, and vacuolar degeneration of cells; The above pathological conditions were significantly improved in the NaF + NaB group (microscopic images of liver slices stained with hematoxylin and eosin (HE), The scale bar representatives 100 μ m).

3.5. Effects of NaF and NaB on liver function

AST and ALT enzyme activities, which are important indicators of liver function, were tested to investigate the effect of NaB on NaF-induced liver function damage. As shown in Table 4, compared with the control group, the NaF group showed significantly higher aminotransferase activity ($p < 0.01$), suggesting the occurrence of liver function injury; compared with the aminotransferase activity in the NaF group, that in the NaF + NaB group was significantly lower ($p < 0.01$), suggesting that NaB can ameliorate the hepatotoxicity induced by NaF.

3.6. Effects of NaF and NaB on antioxidant status

The ameliorative effect of NaB on NaF-induced oxidative damage was explored by analyzing the enzymatic activities of SOD, CAT, and the content of MDA. As shown in Table 4, compared with the control group, the level of MDA was significantly higher in the NaF group, whereas the enzyme activities of SOD and CAT were significantly lower ($P < 0.01$), indicating that NaF induced higher oxidative stress in rats. Compared with those in the NaF group, MDA levels were reduced, and SOD and CAT enzyme activities were significantly increased ($P < 0.01$) in the NaF + NaB group. This indicated that NaB has antioxidant activity in liver tissue and could improve NaF-induced oxidative stress.

3.7. Effects of NaF and NaB on the level of apoptosis

To observe the regulatory effect of NaB on NaF-induced apoptosis, TUNEL staining on rat liver tissues was performed; the results are shown in Fig. 2A and B. Compared with the control group, the apoptotic cells in the NaF group significantly increased ($P < 0.01$). Compared with the NaF group, the NaF +NaB group reduced the degree of cell apoptosis ($P < 0.01$). These results indicate that NaB improves cell apoptosis induced by NaF exposure.

3.8. Effects of NaF and NaB on mitophagy

Transmission electron microscopy was used to observe autophagic vesicles in rat liver tissues. The results are shown in Fig. 3A–D. Among the four groups, only the NaF group exhibited autophagosomes.

3.9. Effects of NaF and NaB on mitophagy markers

To further demonstrate the regulatory effect of NaB on NaF-induced mitochondrial autophagy, we take the RT-qPCR to assess the mRNA levels of the autophagy markers Beclin-1, LC3B, and P62. Compared with the control group, the mRNA levels of Beclin1 and LC3B in the NaF group were significantly increased, whereas the P62 was significantly decreased. However, compared with the NaF group, mRNA levels of Beclin1 and LC3B in the NaF +NaB group were significantly decreased, whereas the mRNA level of P62 was significantly increased (Fig. 4A–C).

Western blotting was used to detect the mitochondrial autophagy-related protein Beclin-1 P62、LC3α/β。 The results are consistent with the RT-qPCR. Compared with the control group, the expression levels of Beclin-1 and LC3 α/β proteins in the liver tissue of NaF group rats were significantly increased, while the expression level of P62 protein was significantly decreased. However, the protein expression levels of these factors returned to normal levels in the NaF +NaB group (Fig. 4D–I). This indicates that NaB can reduce excessive NaF-induced mitophagy.

4. Discussion

Fluoride is one of the most reactive non-metallic elements and adversely affects human health. Studies have shown that high fluoride concentrations exist in the soil at levels ranging from 200 to 300 mg/kg. During irrigation, fluoride in the soil is released into the groundwater, resulting in significantly elevated fluoride levels in some areas. For instance, in certain areas of India and Korea, fluoride concentrations in groundwater reach as high as 40 mg/L(Oliveira Chagas et al., 2023; Solanki et al., 2022; Yadav et al., 2019). Since the renal excretion rate of rats is higher than that of humans, leading to lower fluoride residue in the body, 100 mg/L of NaF was selected for this experiment, based on prior research.

Fluoride can cause damage to multiple systems of the body. Numerous studies have focused on the skeletal system and confirmed that excessive fluoride intake leads to fluoride deposition in bones, altering bone density and causing conditions such as osteosclerosis and osteoporosis (Qiao et al., 2021; Do et al., 2020). Research has demonstrated that the toxic effects of fluoride affect non-skeletal systems, including the liver, kidneys (Malin et al., 2019), and nervous system (Bittencourt et al., 2023). This toxicity can trigger adverse effects such as oxidative stress, mitochondrial dysfunction, and apoptosis (Avila-Rojas et al., 2022; Dong et al., 2024). Excessive NaF has been shown to induce mitochondrial dysfunction in hepatocytes and activate abnormal mitophagy. NaB has been shown to effectively regulate mitophagy in neurological disorders; However, the mechanism that how NaB regulates NaF -induced hepatic histopathology remains unclear. In this study, the protective effects and specific molecular mechanisms of NaB on NaF-induced oxidative stress, apoptosis, and mitophagy were investigated.

Liver is essential for maintaining numerous physiological functions in the human body, regulating the immune and endocrine systems, and ensuring lipid and cholesterol homeostasis. Its primary role is to decompose and metabolize toxic substances absorbed (Trefts et al., 2017). Normal liver function is vulnerable to toxins, which can compromise liver function, resulting in abnormal levels of AST and ALT (Rodimova et al., 2023). Studies have shown that excessive fluoride increases hepatic AST and ALT levels, potentially due to increased permeability of mitochondrial membranes (Zhao et al., 2022). Fluoride-induced histopathological liver damage is characterized by vacuolar and granular degeneration, along with disorganized hepatocyte arrangement (Yu et al., 2023). In this study, rats exposed to NaF exhibited significantly elevated hepatic AST and ALT levels, and liver pathological damage induced by NaF was also observed by HE staining. These results suggest that NaF induces severe hepatic dysfunction, which is significantly ameliorated by NaB treatment. These findings suggest that NaB could serve as a therapeutic agent for NaF -induced liver injury. However, the underlying molecular mechanisms remain unclear.

When the balance between oxidative and antioxidant effects in the body is disrupted, it results in the excessive production of ROS and free radicals, which can damage cellular structure and function (Lu et al.,

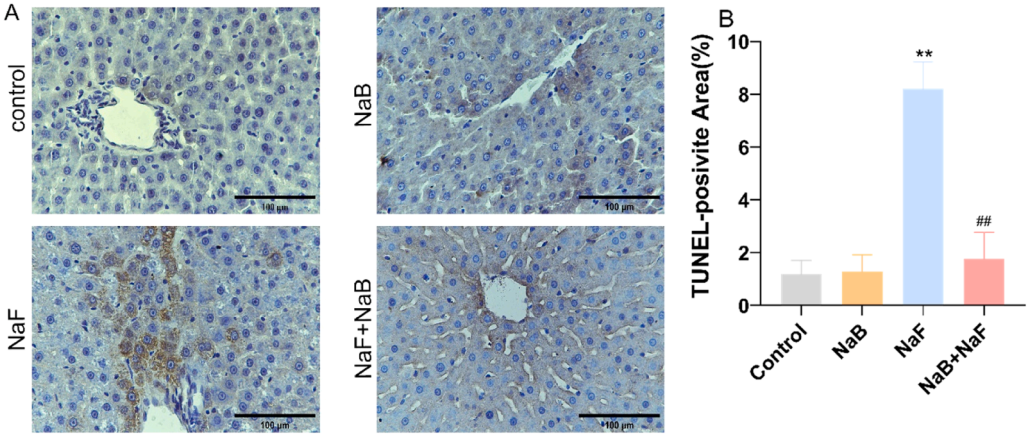

Fig. 2. The effects of NaF and NaB on cell apoptosis. (A) Representative images of TUNEL staining in the liver of different groups of rats (positive for brown granules in the nucleus), Scale bar: 100 μm. Quantification of TUNEL-positive areas in liver tissue samples of rats from different groups (n = 9 samples). (B) Statistical analysis of apoptosis rate of liver cells in four groups of rats. Data were analyzed via one-way ANOVA with the Tukey test. ** $P < 0.01$, compared with Control group; $^{\#\#}$ $P < 0.01$, compared with NaF group.

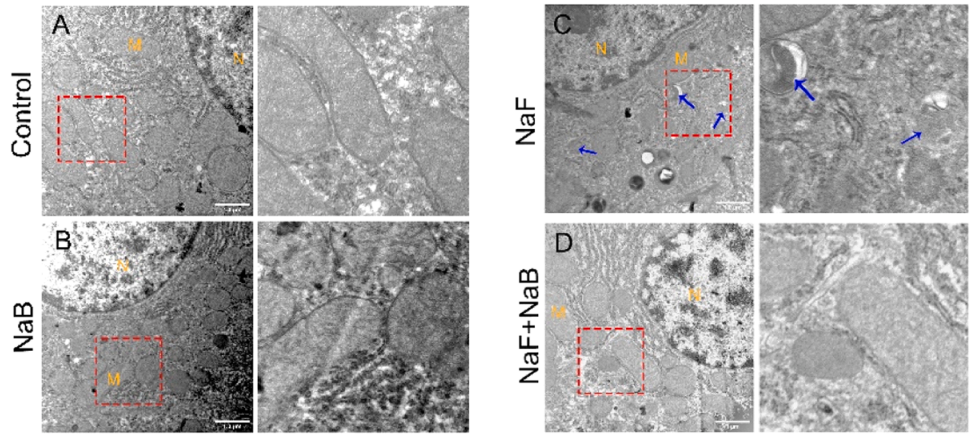

Fig. 3. The effects of NaF and NaB on mitophagy. Representative TEM images of liver tissues from four groups of rats, M: mitochondria, N: nucleus, blue arrows indicate autophagosomes. The scale bar is 1 μm.

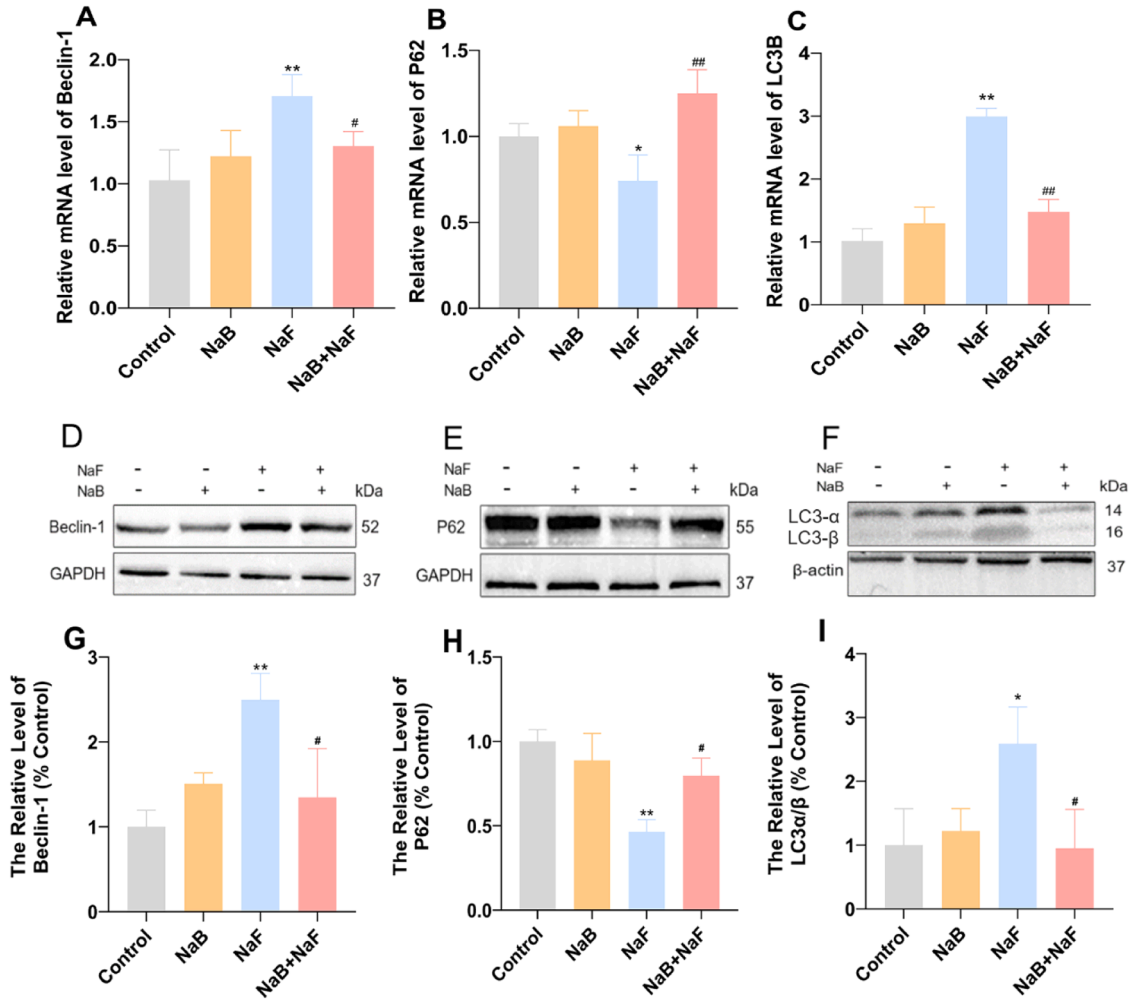

Fig. 4. The effects of NaF and NaB on levels of autophagy markers. (A-C) The effect of NaF and NaB on the mRNA levels of Beclin-1, P62, and LC3B. (D-I) The effect of NaF and NaB on the protein levels of Beclin-1, P62, and LC3 α/β. All data are presented as mean ± SEM. (n = 3). * $P < 0.05$, ** $P < 0.01$, compared with Control group; $^{\#}P < 0.05$, $^{\#\#}P < 0.01$, compared with NaF group.

2017; Zhong et al., 2021). This imbalance is one of the pathogenic mechanisms underlying many diseases, including cancer, cardiovascular diseases, and neurodegenerative disorders (De Los Santos-Jiménez et al., 2025; Kim and Lee, 2024; Anchimowicz et al., 2025; Komal et al., 2025). Fluoride leads to ROS accumulation, which disrupts the balance between ROS and the antioxidant system. This imbalance subsequently causes an increase in MDA levels and a significant decrease in the activity of antioxidant enzymes in the liver (Johnston and Strobel, 2020; Wallace, 2005), ultimately resulting in hepatocellular damage. In this study, NaF increased MDA levels in liver tissues and significantly

decreased the activities of antioxidant enzymes, such as SOD and CAT, disrupting the oxidative stress balance in the liver.

The accumulation of excessive ROS in the body attacks mitochondria, leading to mitochondrial dysfunction. When mitochondrial dysfunction occurs, changes in mitochondrial membrane permeability result in the release of apoptosis-inducing factors such as mitochondrial cytochrome C. Cytochrome C can form apoptotic bodies that bind to the precursor Apaf-1 and ATP/DATP, which subsequently activates caspase-3, triggering a cascade of caspase activation that leads to apoptosis (Xu et al., 2023). Mitophagy, a selective form of autophagy, helps maintain normal mitochondrial function by eliminating damaged mitochondria, preventing the loss of mitochondrial membrane potential, and limiting the release of cytochrome C, thereby reducing apoptosis. Mitophagy can be activated through various signaling pathways, the Pink1-Parkin pathway has been extensively studied (Narendra et al., 2008). When mitochondrial damage occurs, PTEN-induced putative kinase 1 (PINK1) accumulates on the mitochondrial outer membrane and recruits Parkin. Parkin ubiquitinates mitochondrial outer membrane proteins, marking mitochondria as targets for autophagic degradation (Kawajiri et al., 2010). The cell then forms a bilayer membrane structure, known as the isolation membrane or phagophore, progressively engulfs the target mitochondria. LC3 accumulates on the autophagosome membrane, facilitating its extension and closure. P62, via its UBQ domain, recruits ubiquitinated substrates into autophagosomes. The interaction between P62 and LC3 ensures the specific degradation of these substrates, enabling efficient mitochondrial autophagy. These proteins interact synergistically to maintain cellular homeostasis (Lavalle-Carrasco et al., 2024).

Notably, mitophagy can have both beneficial and detrimental effects. Excessive mitophagy can result in the removal of too many normally functioning mitochondria, allowing apoptotic factors to enter the cytoplasm, which can lead to rapid cell death. Studies have shown that in Parkinson's disease, excessive mitophagy contributes to rapid neuronal death (Guo et al., 2016; Huang et al., 2023). Similarly, in Alzheimer's disease, mitochondrial dysfunction coupled with excessive mitophagy leads to a loss of cellular energy, exacerbating neurodegenerative processes (Morikawa et al., 2014). Numerous studies on fluorosis have confirmed that NaF induces excessive mitophagy in neural (Tang et al., 2023), skeletal (Song et al., 2023), and myocardial tissues (Tian et al., 2023), resulting in significant cellular injury. In this study, Transmission electron microscopy and TUNEL detection revealed that excessive NaF led to an increase in autophagic vesicles in liver tissue. Additionally, the protein and mRNA expression levels of P62, LC3, and Beclin-1 were assessed by Western blotting and RT-qPCR, respectively, to evaluate mitophagy initiation. The results demonstrated that excess NaF upregulated the expression of autophagy-related proteins LC3 and Beclin-1, while P62 expression decreased in rat liver, indicating a significant increase in mitophagy and an elevation in apoptotic cells.

NaB is a product of dietary fiber fermentation in the colon. Due to its natural occurrence in the human body and low toxicity, it has gained widespread use in medicine and as a feed additive for regulating intestinal health, promoting intestinal cell development, and enhancing immune function. Research indicates that NaB can alleviate mitochondrial damage induced by oxidative stress via the AMPK-mediated mitophagy pathway (Li et al., 2022), and it also can inhibit autophagy by modulating the PI3K/Akt pathway, thereby mitigating oxidative stress caused by advanced glycation end products (Yan et al., 2022). In this study, NaB mitigates oxidative stress damage induced by NaF. Specifically, NaB reduces the level of MDA in fluoride-poisoned liver tissue and restores the activity of antioxidant enzymes SOD and CAT. Furthermore, the TUNEL assay revealed a reduction in apoptotic cells, indicating that NaB can improve cell apoptosis induced by NaF. Subsequently, we confirmed the decreased expression of Beclin-1 and LC3, and the increased expression of P62, at both the transcriptional and translational levels, demonstrating that NaB attenuates the aberrant mitochondrial autophagy induced by NaF. Overall, these findings suggest that NaB can restore mitochondrial homeostasis by reducing mitochondrial phagocytosis, thereby alleviating oxidative stress and cell apoptosis, and thus recovering the liver damage caused by NaF.

However, this study has limitations. Rats have a highly efficient renal metabolic system that facilitates the excretion of fluoride, leading to relatively low fluoride concentrations in their bodies. Consequently, the fluoride concentration in rats may be significantly lower than that of humans. This discrepancy may be attributed to structural differences in the kidneys and variations in fluoride excretion rates between species. Despite increasing the NaF concentration, further optimization of the experimental design is necessary to address this discrepancy.

5. Conclusion

This study demonstrates that excessive fluoride intake causes pathological liver damage and dysfunction, likely due to oxidative stress, apoptosis, and excessive mitophagy. The study found that NaB alleviated fluoride-induced liver damage in rats by modulating oxidative stress, apoptosis, and excessive mitophagy in the liver tissue. The role of NaB may offer new possibilities for research and therapeutic interventions in fluoride-induced liver injury.

CRediT authorship contribution statement

Meng Lu: Investigation, Data curation. **Duan Xiaoxu:** Software, Data curation. **Wang Zhengdong:** Resources, Funding acquisition, Conceptualization. **Qi Rong:** Investigation, Data curation. **Xu Leiyu:** Validation, Investigation, Data curation. **Yan Nan:** Supervision, Conceptualization. **Sun Zhenxiang:** Methodology, Data curation. **Zhang Xiaolin:** Validation, Software, Writing – review & editing. **Ren Fu:** Supervision, Conceptualization. **Xia Jing:** Writing – original draft, Visualization, Investigation, Data curation.

Declaration of Competing Interest

The authors declare that they have no known competing financial interests or personal relationships that could have appeared to influence the work reported in this paper.

Acknowledgements

This study was supported by the Basic Research Project of Liaoning Provincial Department of Education (JYTMS20231391) to Zhengdong Wang; The Center Guiding Local Science and Technology Foundation of Liaoning Science and Technology Committee (2023JH6/100100021) to Fu Ren; The Team Construction Project of Liaoning Province Education Department (LJ222410164002) to Nan Yan; The Liaoning Provincial Science and Technology Project Innovation Ability Improvement Joint Fund (2022-NLTS-14-06) to Nan Yan; The 2022 Basic Scientific Research of the Liaoning Education Department (LJKM720221792) to Xiaolin Zhang.

Data availability

Data will be made available on request.

References

Aguilar-Díaz, F.D.C., Morales-Corona, F., Cintra-Viveiro, A.C., et al., 2017. Prevalence of dental fluorosis in Mexico 2005-2015: a literature review. Salud Publica De. Mex. 59 (3), 306–313.

Anchimowicz, J., Zielonka, P., Jakiela, S., 2025. Plant secondary metabolites as modulators of mitochondrial health: an overview of their anti-oxidant, anti-apoptotic, and mitophagic mechanisms. Int J. Mol. Sci. 26 (1).

Avila-Rojas, S.H., Aparicio-Trejo, O.E., Sanchez-Guerra, M.A., et al., 2022. Effects of fluoride exposure on mitochondrial function: energy metabol ism, dynamics, biogenesis and mitophagy. Environ. Toxicol. Pharmacol. 94, 103916.

Bittencourt, L.O., Dionizio, A., Ferreira, M.K.M., et al., 2023. Prolonged exposure to high fluoride levels during adolescence to adult hood elicits molecular, morphological, and functional impairments in t he hippocampus. Sci. Rep. 13 (1), 11083.
Chang, P.V., Hao, L., Offermanns, S., et al., 2014. The microbial metabolite butyrate regulates intestinal macrophage func tion via histone deacetylase inhibition. Proc. Natl. Acad. Sci. 111 (6), 2247–2252.
De Los Santos-Jiménez, J., Campos-Sandoval, J.A., Rosales, T., et al., 2025. Glutaminase-2 expression induces metabolic changes and regulates pyruvate dehydrogenase activity in glioblastoma cells. Int J. Mol. Sci. 26 (1).
Do, L.G., Ha, D.H., Roberts-Thomson, K.F., et al., 2020. Dental fluorosis in the Australian adult population. Aust. Dent. J. 65 (1), S47–S51.
Dong, Y., Sun, X., He, W., et al., 2024. Elevated Level of PINK1/Parkin-mediated mitophagy pathway involved to the inhibited activity of mitochondrial superoxide dismutase in rat br ains and primary hippocampal neurons exposed to high level of fluoride. Biol. Trace Elem. Res. 202 (2), 538–547.
Dong, Y., Sun, X., He, W., et al., 2024. Elevated level of PINK1/Parkin-mediated mitophagy pathway involved to the inhibited activity of mitochondrial superoxide dismutase in rat brains and primary hippocampal neurons exposed to high level of fluoride. Biol. Trace Elem. Res 202 (2), 538–547.
Duan, Q., Jiao, J., Chen, X., et al., 2018. Association between water fluoride and the level of children's intelli gence: a dose-response meta-analysis[J]. Public Health 154, 87–97.
Feng, F., Jia, Y., Yang, Y., et al., 2020. Hydrogeochemical and statistical analysis of high fluoride groundwater in northern China. Environ. Sci. Pollut. Res. Int. 27 (28), 34840–34861.
Garza-Lombó, C., Pappa, A., Panayiotidis, M.I., et al., 2020. Redox homeostasis, oxidative stress and mitophagy. Mitochondrion 51, 105–117.
Gu, S., Zheng, X., Gao, X., et al., 2024. Cadmium-induced oxidative damage and the expression and function of mitochondrial thioredoxin in phascolosoma esculenta. Int J. Mol. Sci. 25 (24).
Guo, X., Sun, X., Hu, D., et al., 2016. VCP recruitment to mitochondria causes mitophagy impairment and neurod egeneration in models of Huntington's disease. Nat. Commun. 7, 12646.
Hu, Y., Li, Y., Li, M., et al., 2024. Calcium supplementation attenuates fluoride-induced bone injury via PINK1/Parkin-mediated mitophagy and mitochondrial apoptosis in mice. J. Hazard Mater. 465, 133411.
Huang, Y., Liang, B., Li, Z., et al., 2023. Polystyrene nanoplastic exposure induces excessive mitophagy by activa ting AMPK/ULK1 pathway in differentiated SH-SY5Y cells and dopaminergi c neurons in vivo. Part. Fibre Toxicol. 20 (1), 44.
Hung, M., Hon, E.S., Mohajeri, A., et al., 2023. A national study exploring the association between fluoride levels and dental fluorosis. JAMA Netw. Open 6 (6), e2318406.
Johnston, N.R., Strobel, S.A., 2020. Principles of fluoride toxicity and the cellular response: a review. Arch. Toxicol. 94 (4), 1051–1069.
Kawajiri, S., Saiki, S., Sato, S., et al., 2010. PINK1 is recruited to mitochondria with parkin and associates with LC3 in mitophagy. FEBS Lett. 584 (6), 1073–1079.
Kim, T.W., Lee, H.G., 2024. Anti-inflammatory 8-shogaol mediates apoptosis by inducing oxidative stress and sensitizes radioresistance in gastric cancer. Int. J. Mol. Sci. 26 (1).
Komal, K., Ghosh, R., Sil, D., et al., 2025. Advancements in nose-to-brain drug targeting for Alzheimer's disease: a review of nanocarriers and clinical insights. Inflammopharmacology.
Lavalle-Carrasco, J., Molina-Frechero, N., López-Verdín, S., et al., 2024. Health implications of proinflammatory cytokine activity at different levels of fluoride exposure: a systematic review. J. Appl. Toxicol.
Li, Y., Wang, Z., Li, J., et al., 2023. Sodium butyrate ameliorates fluorosis-induced neurotoxicity by regulat ing hippocampal glycolysis in vivo. Biol. Trace Elem. Res. 201 (11), 5230–5241.
Li, Y., Wang, Z., Li, J., et al., 2023. Sodium butyrate ameliorates fluorosis-induced neurotoxicity by regulating hippocampal glycolysis in vivo. Biol. Trace Elem. Res 201 (11), 5230–5241.
Li, X., Wang, C., Zhu, J., et al., 2022. Sodium butyrate ameliorates oxidative stress-induced intestinal epithe lium barrier injury and mitochondrial damage through AMPK-mitophagy pathway. Oxid. Med. Cell. Longev. 2022, 3745135.
Liu, S., Yu, X., Xing, Z., et al., 2024. The impact of exposure to iodine and fluorine in drinking water on thyroid health and intelligence in school-age children: a cross-sectional investigation. Nutrients 16 (17).
Lu, Y., Luo, Q., Cui, H., et al., 2017. Sodium fluoride causes oxidative stress and apoptosis in the mouse liver. Aging 9 (6), 1623–1639.
Malin, A.J., Lesseur, C., Busgang, S.A., et al., 2019. Fluoride exposure and kidney and liver function among adolescents in t he United States: NHANES, 2013-2016. Environ. Int. 132, 105012.
Martignon, S., Bartlett, D., Manton, D.J., et al., 2021. Epidemiology of erosive tooth wear, dental fluorosis and molar incisor hypomineralization in the american continent. Caries Res. 55 (1), 1–11.
Morikawa, K., Tsuji, T., Yamasaki, H., et al., 2014. Paraneoplastic pemphigus occurs most commonly in indolent B cell lymphoma. Acta Haematol. 132 (1), 73–74.
Narendra, D., Tanaka, A., Suen, D.-F., et al., 2008. Parkin is recruited selectively to impaired mitochondria and promotes their autophagy. J. Cell Biol. 183 (5), 795–803.
Oliveira Chagas, F., Rocha Valadas, L.A., Sorazabal, A., et al., 2023. Fluoride in drinking groundwater and prevalence of fluorosis in children and adolescents: a systematic review. Acta Odontol. Latinoam.: AOL 36 (3), 169–176.
O'mullane, D.M., Baez, R.J., Jones, S., et al., 2016. Fluoride and oral health. Community Dent. Health 33 (2), 69–99.
Park J.-S., Lee E.-J., Lee J.-C., et al. Anti-inflammatory effects of short chain fatty acids in IFN-gamma-stim ulated RAW 264.7 murine macrophage cells: involvement of NF-kappaB and ERK signaling pathways[J]. International immunopharmacology, 7(1): 70-77.
Qiao, L., Liu, X., He, Y., et al., 2021. Progress of signaling pathways, stress pathways and epigenetics in the pathogenesis of skeletal fluorosis. Int. J. Mol. Sci. 22 (21), 11932.
Rodimova, S., Mozherov, A., Elagin, V., et al., 2023. Effect of hepatic pathology on liver regeneration: the main metabolic mechanisms causing impaired hepatic regeneration. Int. J. Mol. Sci. 24 (11), 9112.
Smith, G.E., 1988. Fluoride and fluoridation. Soc. Sci. Med. 26 (4), 451–462.
Solanki, Y.S., Agarwal, M., Gupta, A.B., et al., 2022. Fluoride occurrences, health problems, detection, and remediation meth ods for drinking water: a comprehensive review. Sci. Total Environ. 807 (Pt 1), 150601.
Song, C., Zhang, A., Zhang, M., et al., 2023. Nrf2/PINK1-mediated mitophagy induction alleviates sodium fluoride-induced hepatic injury by improving mitochondrial function, oxidative stress, and inflammation. Ecotoxicol. Environ. Saf. 252, 114646.
Song, C., Zhang, A., Zhang, M., et al., 2023. Nrf2/PINK1-mediated mitophagy induction alleviates sodium fluoride-ind uced hepatic injury by improving mitochondrial function, oxidative str ess, and inflammation. Ecotoxicol. Environ. Saf. 252, 114646.
Tang, Y., Zhang, J., Hu, Z., et al., 2023. PRKAA1 induces aberrant mitophagy in a PINK1/Parkin-dependent manner, contributing to fluoride-induced developmental neurotoxicity. Ecotoxicol. Environ. Saf. 255, 114772.
Tian, X., Wang, M., Ying, X., et al., 2023. Co-exposure to arsenic and fluoride to explore the interactive effect on oxidative stress and autophagy in myocardial tissue and cell. Ecotoxicol. Environ. Saf. 253, 114647.
Tian, H.Y., Yu, D.J., Xie, T., et al., 2025. Cordycepin alleviates metabolic dysfunction-associated liver disease by restoring mitochondrial homeostasis and reducing oxidative stress via Parkin-mediated mitophagy. Biochem Pharm., 116750
Trefts, E., Gannon, M., Wasserman, D.H., 2017. The liver. Curr. Biol.: CB 27 (21), R1147–R1151.
Wallace, D.C., 2005. A mitochondrial paradigm of metabolic and degenerative diseases, aging, and cancer: a dawn for evolutionary medicine. Annu. Rev. Genet. 39, 359–407.
Wang, T., Li, H., Li, Y., et al., 2024. Selenomethionine supplementation mitigates fluoride-induced liver apoptosis and inflammatory reactions by blocking Parkin-mediated mitophagy in mice. Sci. Total Environ. 951, 175458.
Wang, H.-W., Miao, C.-Y., Liu, J., et al., 2020. Fluoride-induced rectal barrier damage and microflora disorder in mice. Environ. Sci. Pollut. Res. Int. 27 (7), 7596–7607.
Watchon, M., Robinson, K.J., Luu, L., et al., 2024. Treatment with sodium butyrate induces autophagy resulting in therapeutic benefits for spinocerebellar ataxia type 3. Faseb J. 38 (2), e23429.
Waugh, D.T., 2019. The contribution of fluoride to the pathogenesis of eye diseases: mole cular mechanisms and implications for public health. Int. J. Environ. Res. Public Health 16 (5), 856.
Wen, J., Xu, Q., Li, J., et al., 2024. Sodium butyrate exerts a neuroprotective effect in rats with acute carbon monoxide poisoning by activating autophagy through the mTOR signaling pathway. Sci. Rep. 14 (1), 4610.
Xu, W., Hu, Z., Zhang, J., et al., 2023. Cross-talk between autophagy and ferroptosis contributes to the liver injury induced by fluoride via the mtROS-dependent pathway. Ecotoxicol. Environ. Saf. 250, 114490.
Xue, D., Cheng, Y., Pang, T., et al., 2023. Sodium butyrate alleviates deoxynivalenol-induced porcine intestinal b arrier disruption by promoting mitochondrial homeostasis via PCK2 signaling. J. Hazard. Mater. 459, 132013.
Yadav, K.K., Kumar, S., Pham, Q.B., et al., 2019. Fluoride contamination, health problems and remediation methods in Asi an groundwater: a comprehensive review. Ecotoxicol. Environ. Saf. 182, 109362.
Yan, M., Li, X., Sun, C., et al., 2022. Sodium butyrate attenuates AGEs-induced oxidative stress and inflammat ion by inhibiting autophagy and affecting cellular metabolism in THP-1 cells. Molecules 27 (24), 8715.
Yu, Y., Xu, J., Li, H., et al., 2023. α-Lipoic acid improves mitochondrial biogenesis and dynamics by enhancing antioxidant and inhibiting Wnt/Ca(2+) pathway to relieve fluoride-induced hepatotoxic injury. Chem. Biol. Inter. 385, 110719.
Zhao, Y., Wang, J., Zhang, J., et al., 2022. Fluoride exposure induces mitochondrial damage and mitophagy via activ ation of the IL-17A pathway in hepatocytes. Sci. Total Environ. 804, 150184.
Zhong, N., Yao, Y., Ma, Y., et al., 2021. Effects of fluoride on oxidative stress markers of lipid, gene, and pr otein in rats. Biol. Trace Elem. Res. 199 (6), 2238–2246.
Zhou, D., Pan, Q., Xin, F.-Z., et al., 2017. Sodium butyrate attenuates high-fat diet-induced steatohepatitis in mi ce by improving gut microbiota and gastrointestinal barrier. World J. Gastroenterol. 23 (1), 60–75.
Zong, Q., Li, K., Qu, H., et al., 2023. Sodium butyrate ameliorates deoxynivalenol-induced oxidative stress an d inflammation in the porcine liver via NR4A2-mediated histone acetyla tion. J. Agric. Food Chem. 71 (27), 10427–10437.

Glossary

Abbreviation: Title
NaF: Sodium fluoride
NaB: Sodium butyrate
AST: Aspartate aminotransferase
ALT: Alanine aminotransfease
SOD: Superoxide dismutase
CAT: Catalase
MDA: Malondialdehyde
P62: Sequestosome 1
LC3: MAP1LC3
ROS: reactive oxygen species

OD: optical density
PH: Potential of hydrogen
DNPH: 2,4-dinitrophenylhydrazine
RIPA: Radioimmunoprecipitation assay buffer
PMSF: Phenylmethanesulfonyl fluoride
BCA: BCA assay
PVDF: Polyvinylidene fluoride
WB: Western blotting
rpm: Revolutions Per minute
mRNA: messenger RNA
SDS: Sodium dodecyl sulfate
ECL: Enhanced chemiluminescence
GAPDH: Glyceraldehyde-3-phosphate dehydrogenase
RT-qPCR: Real time-quantitative PCR
H_2O_2: Hydrogen Peroxide
HE: Hematoxylin-eosin staining
DAB: 3,3′-Diaminobenzidine
HRP: Horseradish Peroxidase
TEM: Transmission Electron Microscopy
mg: Milligram
kg: Kilogram
cm: Curium
h: Hour
g: Gram
μL: Microliter
mL: Milliliter
min: Minute